Electronic structures and local atomic configurations in amorphous GeSe and GeTe

Electronic structures and local atomic configurations in amorphous GeSe and GeTe

S Hosokawa†‖, Y Hari†, T Kouchi†, I Ono†, H Sato†, M Taniguchi†,
A Hiraya†, Y Takata‡, N Kosugi‡ and M Watanabe§

† Department of Materials Science, Faculty of Science, Hiroshima University, Higashi-Hiroshima
739, Japan
‡ Institute for Molecular Science, Okazaki 444, Japan
§ Research Institute for Scientific Measurements, Tohoku University, Sendai 980, Japan

Abstract. The valence- and conduction-band electronic densities of states (DOSs) in amorphous (a-) GeSe and GeTe were investigated by means of ultraviolet photoemission and inverse-photoemission spectroscopy (UPS and IPES), respectively. The UPS spectra for both a-GeSe and a-GeTe are very similar to those obtained in previous experiments; a distinct peak appears near the top of the valence band. The IPES spectra for both a-GeSe and a-GeTe corrected by subtracting the background exclude the possibility of a structure with 3(Ge):3(chalcogen) coordination if one compares them with the theoretical DOS calculated by O'Reilly, Robertson and Kelly. The corrected IPES spectrum for a-GeSe resembles the broadened theoretical DOS for *chemically ordered* 4(Ge):2(Se) structure, whereas that for a-GeTe resembles the theoretical DOS for *randomly bonded* 4(Ge):2(Te) structure. The characters of the conduction-band DOSs for a-GeSe and a-GeTe were also examined by means of soft-x-ray core absorption spectroscopy. The Ge and Se $2p_{3/2}$ core absorption spectra of a-GeSe are very similar to those of a-GeSe$_2$, and were discussed using a simple bonding model with a 4(Ge):2(Se) local configuration. The Ge $2p_{3/2}$ and Te $3p_{3/2}$ core absorption spectra of a-GeTe were also discussed using a simple local bonding model. All of the present measurements indicate that both a-GeSe and a-GeTe have structures with 4(Ge):2(chalcogen) coordination.

1. Introduction

In crystalline (c-) GeSe with an orthorhombic form, threefold-coordinated Ge atoms and threefold-coordinated Se atoms are bonded to each other and form a layer structure [1] as shown schematically in figure 1. On the other hand, c-GeTe has a rhombohedral structure distorted slightly from a NaCl-type one, in which the Ge and Te atoms form three short bonds (solid lines) and three long bonds (dashed lines) with each other [2] as shown schematically in figure 2. The coordinations of the individual elements in these crystals do not follow the well-known $8 - N$ rule.

The short-range order of amorphous (a-) GeSe has been studied by many investigators for more than two decades, but there is still considerable controversy over whether it has a structure with 3(Ge):3(Se) coordination like c-GeSe or one with 4(Ge):2(Se) coordination like c-GeSe$_2$ and a-GeSe$_2$. The leading extended x-ray absorption fine-structure (EXAFS) study by Sayers, Lytle and Stern [3] carried out in 1972 reported a considerable change in

‖ Present address: Institute of Physical, Nuclear, and Macromolecular Chemistry, Philipps University of Marburg, D-35032 Marburg, Germany.
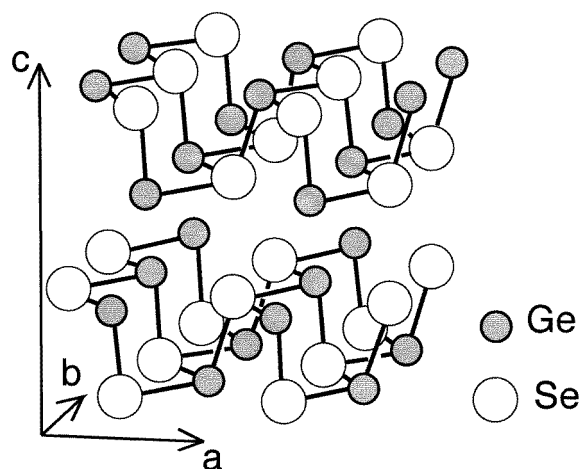
Figure 1. Schematic views of the crystal structure of orthorhombic GeSe. Small grey and large empty circles indicate Ge and Se atoms, respectively.
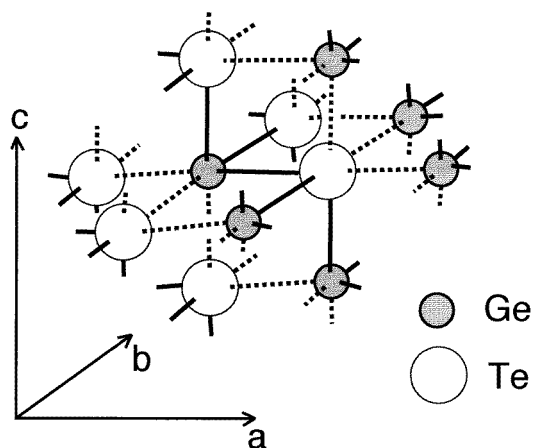

Figure 2. Schematic views of the crystal structure of rhombohedral GeTe. Small grey and large empty circles indicate Ge and Te atoms, respectively. Solid and dashed lines show the short and long bonds, respectively.

the local structures around both the Ge and Se atoms on going from c-GeSe to a-GeSe: the first-nearest neighbours split into two, the bond length of the shorter ones shrinks by more than 0.2 Å and the coordination number of the Se atoms reduces to two. Sayers *et al* deduced that a-GeSe had a somewhat distorted covalent bonding arrangement of the nearest neighbours. A similar deduction was made on the basis of the x-ray measurements by Uemura, Sagara and Satow [4]. In contrast, Fuoss *et al* [5] performed the pioneering work of making an anomalous x-ray scattering measurement using synchrotron radiation, and obtained the results that the coordination number N_1 for the Ge atoms is 3.1 and that N_1 for the Se atoms is 2.5. Therefore, they deduced that a structure with 3(Ge):3(Se) coordination was more probable. The later EXAFS measurement by Oyanagi *et al* [6] also supported the proposal of a 3(Ge):3(Se) local structure.

Kawamura and Matsumura [7] took Raman scattering spectra for a-Ge_xSe_{1-x} mixtures in the concentration range $x = 0$–0.7. The spectral change on going from $x = 0.45$ to $x = 0.5$ is remarkable: two peaks originating from $Ge(Se_{1/2})_4$ tetrahedral units suddenly disappear and two new peaks appear in the low-wavenumber region. They proposed that the new peaks were due to structure with 3(Ge):3(Se) coordination in a-GeSe. However, the far-infrared data [8, 9] showed not an absorption peak which is characteristic of 3(Ge):3(Se) coordination for c-GeSe, but a clear absorption peak which was assigned to a $Ge(Se_{1/2})_4$ tetrahedral vibration mode in a-$GeSe_2$ with 4(Ge):2(Se) coordination.

From the viewpoint of the electronic structure, O'Reilly, Robertson and Kelly [10] calculated the density of states (DOS) for a-GeSe on the basis of both 3(Ge):3(Se) and 4(Ge):2(Se) coordination models. They found that these models gave very similar multiple-peaked p-bonding bands at the top of the valence bands to each another, and that only the valence Ge 4s bands were very sensitive to changes in the local order, particularly to the presence of homopolar bonds. They made a comparison with an experimental result obtained by means of ultraviolet photoemission spectroscopy (UPS) by Hino, Takahashi and Harada [11], and concluded that the structure with 3(Ge):3(Se) coordination could be inferred for a-GeSe. However, the difference in the calculated DOSs between these models was very small except as regards the Ge 4s level, and, in addition, the UPS data did not provide reliable evidence because the details of the valence bands for a region with such high binding energy were obscured due to the rapidly rising background of secondary electrons.

Oyanagi *et al* [6] investigated the local structure of a-GeSe by means of x-ray photo-emission spectroscopy (XPS) and concluded that the spectrum obtained did not contradict the 3(Ge):3(Se)-coordinated structure model suggested by O'Reilly, Robertson and Kelly [10]. Takahashi and Sagawa [12] took UPS and XPS spectra, varying the substrate temperature during the sample evaporation. They based their arguments on the sharpness of the Ge and Se s peaks in the spectra and found that the local structure strongly depended on the sample preparation conditions. However, the recent XPS spectrum for a-GeSe taken by Theye *et al* [13] revealed a broadening and flattening of the Ge 4s band resulting from the presence of a substantial proportion of Ge–Ge bonds. Theye *et al* also investigated the shift and broadening of the Ge and Se 3d core levels, which seemed to confirm that 4(Ge):2(Se) coordination was most likely.

For a-GeTe, on the other hand, the situation is not so controversial as it is for a-GeSe. The structural x-ray diffraction studies made by Betts, Bienenstock and Ovshinsky [14] in 1970 revealed that the interatomic distance and the coordination number of a-GeTe are in poor agreement with those of c-GeTe. From detailed analysis of the peak, they concluded that a random covalent model with a 4(Ge):2(Te) local coordination was the most appropriate as a local coordination model for a-GeTe. The later electron diffraction studies [15, 16] obtained similar radial distribution functions. Only the neutron scattering result of [17] suggested a 3(Ge):3(Te)-coordinated local structure due to the small coordination number obtained. The 4(Ge):2(Te)-coordinated structure was also suggested on the basis of an EXAFS measurement around the Ge K edge made by Maeda and Wakagi [18].

Raman scattering and far-infrared absorption spectra for a-GeTe were taken by Fisher, Tauc and Verhelle [19] and were explained in terms of the presence of $GeTe_4$ tetrahedra. Their results strongly supported a random covalent network model of the 4(Ge):2(Te)-coordinated atoms, and excluded the possibility of a c-GeTe microcrystalline structure. Besides the neutron scattering measurement of [17], a 3(Ge):3(Te) local structure of a-GeTe was only supported by the Mössbauer spectrometry of ^{125}Te nuclei performed by Boolchand *et al* [20].

Fisher *et al* [21, 22] obtained valence-band spectra by means of UPS and XPS, and

found a distinct peak at the top of the valence p band together with the broadening of the Ge s band. The peak in the valence p band was not observed for 3(Ge):3(Se)-coordinated c-GeTe, which was attributed to a lone-pair orbital of twofold-coordinated Te atoms. At almost the same time, Shevchik *et al* [23, 24] took UPS and XPS spectra and found that each spectrum was similar to the sum of the spectra for the elements Ge and Te. Thus, they inferred that their results supported a random covalent structural model. Takahashi *et al* [12, 25] took UPS and XPS spectra varying the substrate temperature during the sample evaporation, and found that the local structure strongly depended on the sample preparation conditions. O'Reilly, Robertson and Kelly [10] pointed out that the peak in the valence p band did not indicate the existence of Te lone-pair states, in accordance with their band calculation. Nevertheless, they interpreted the weakening of the Ge s peak and the slight dip between the Te and Ge s bands in the XPS spectrum as providing evidence of a *chemically ordered* 4(Ge):2(Te)-coordinated structure. It should be noted that there is still ambiguity as regards whether the network is *chemically ordered* with no Te–Te bond allowed or randomly bonded with the proportions of Ge–Ge, Ge–Te and Te–Te bonds determined statistically, though the 4(Ge):2(Te) model has been the choice of the majority for describing the local coordination in a-GeTe.

As shown above, there is no doubt that the electronic structure of amorphous material is a good probe for obtaining important information on its local structure, which not only compensates for the inadequate results of structural diffraction experiments, but also provides crucial results as regards its local atomic configuration. However, previous studies were almost all limited to investigating the valence-band DOS using the photoemission technique. Inverse-photoemission spectroscopy (IPES) provides direct information on the conduction-band DOS. Core absorption spectroscopy also supplies it, in particular, including the selection rule for the angular momentum on the optical transitions. By comparing core absorption spectra with IPES spectra, we can extract the contribution of each orbital component from the conduction-band DOS, which would be a strong probe of the unoccupied electronic states.

In this paper, we report the results of UPS, IPES and soft-x-ray core absorption measurements for a-GeSe and a-GeTe. In carrying out these experiments we concentrate on making clear the conduction-band DOS and the contributions of the orbital components such as those of the s, p and d orbitals in a-GeSe and a-GeTe, and we discuss the local coordination of each constituent element on the basis of the electronic structure.

2. Experimental procedures

2.1. Ultraviolet photoemission and inverse-photoemission spectroscopy

Figure 3 shows a schematic diagram of the apparatus used for recording the UPS and IPES spectra. It is mainly composed of four ultrahigh-vacuum chambers: two chambers for the sample preparation, an IPES analyser one and an UPS analyser one, operating under base pressures of 4.0×10^{-10}, 7.0×10^{-11} and 8.0×10^{-10} Torr, respectively.

In the IPES chamber, a monoenergetic electron beam from an electron gun of Erdman–Zipf type with a BaO cathode, which can deliver a high beam current down to low kinetic energy (1–10 μA at 10 eV) and has an energy spread of 0.25 eV, was focused onto the sample. Light emitted from the sample was focused by an Al reflection mirror coated with a MgF$_2$ film and detected using a bandpass photon detector of our own design [26]. The detector consists basically of a simple combination of a pure SrF$_2$ entrance window and a commercial Cu–BeO photomultiplier. Evaporation of KCl onto the first dynode of the

Bandpass
Photon Detector

He Discharge Lamp

Sample Bank

GV

Transfer Rod

GV

GV

GV

DCMA

Au Source

Channeltron   Electron Gun

Al Reflection Mirror

GeSe(GeTe) Source

UPS   IPES

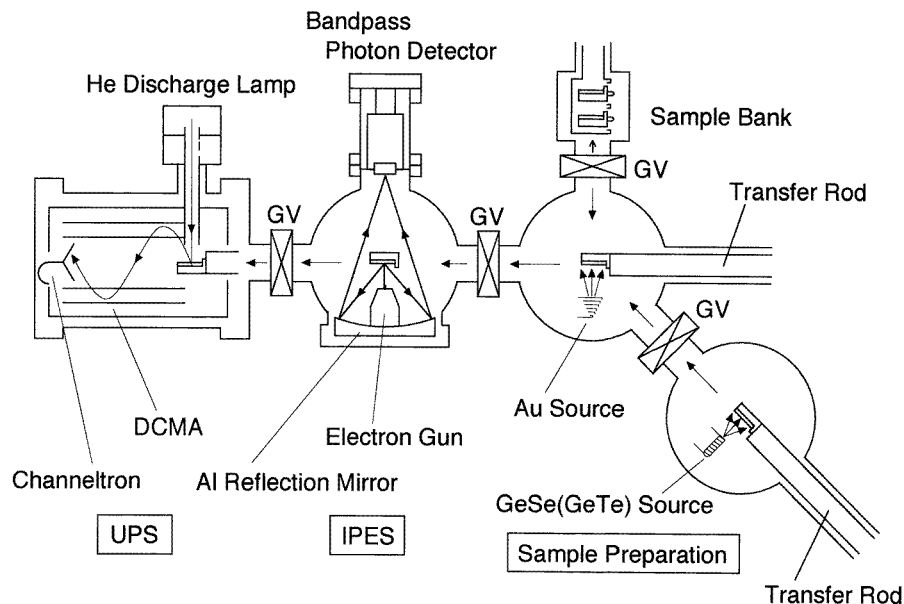Sample Preparation

Transfer Rod

Figure 3. A schematic diagram of the IPES and UPS spectrometer used for studying a-GeSe and a-GeTe. GV: gate valve.

photomultiplier improved the bandpass characteristics and the sensitivity. The full width at half-maximum of the detector was 0.47 eV centred at 9.43 eV and the sensitivity was increased by about one order of magnitude in comparison with the original one. The overall energy resolution of the spectrometer was 0.56 eV [27]. The UPS spectrometer was composed of a He discharge lamp ($h\nu = 21.2$ eV) as an excitation light source and a double-stage cylindrical-mirror analyser (DCMA) as an electron energy analyser for obtaining angle-integrated spectra. The energy resolution of the UPS spectrometer was set to be 0.2 eV. The energy calibrations of the IPES and UPS spectra were performed experimentally using the spectra of the fresh polycrystalline Au film.

The a-GeSe film was prepared *in situ* by evaporating a source crystal onto a Au film, which was evaporated onto a Cu substrate and is inactive against a-GeSe, in one of the preparation chambers, using a quartz furnace under a vacuum of about 1.5×10^{-9} Torr during the evaporation. The a-GeTe sample film was evaporated onto a Mo substrate in the preparation chamber. We used commercial samples with purity of 99.9999% as starting materials. The purity of the Au source was 99.99%. The sample thickness was set to be around 70 Å in order to prevent the IPES signal from charging the sample when it was too thick and from mixing the signal from the substrate when it was too thin [28]. The thickness was measured by means of deviations of the frequency of the quartz oscillator placed near the sample position. The evaporation rate for each film was set at 0.1–0.2 Å s^{-1} in order to conserve the stoichiometry of the sample. Because the samples were so thin and on a crystalline metal substrate, we could not directly check that they included no small crystal grains. Therefore we separately made thick samples on glass substrates under the same evaporating conditions and checked them using an x-ray diffractometer.

Clean surfaces of c-GeSe and c-GeTe were obtained by scraping polycrystalline lumps using a diamond file in the preparation chamber under an ultrahigh vacuum of about

3.0×10^{-10} Torr. We tried to prepare c-GeSe using a high-temperature substrate beyond its crystallization temperature, but did not obtain a c-GeSe thin film because of re-evaporation from the substrate. Therefore, we could not take an IPES spectrum for c-GeSe without the sample charging. The concentrations of the samples were later examined by means of an electron microprobe analysis with an uncertainty of a few per cent. The samples were immediately transferred into the analyser chamber under an ultrahigh vacuum below 2.0×10^{-10} Torr. We carefully checked the contamination of the samples during the measurements by observing the changes of both the UPS and IPES spectra repeatedly, because the typical effect of the contaminants appears in the DOS of both the bonding and antibonding states. No deformation of the spectra appeared within our measuring time of about two days.

2.2. Soft-x-ray core absorption spectroscopy

The Ge $2p_{3/2}$, Se $2p_{3/2}$ and Te $3p_{3/2}$ core absorption spectra were taken at the soft-x-ray beamline (BL-1A) of UVSOR at the Institute for Molecular Science. A schematic diagram of the apparatus for the core absorption measurements was given as figure 1 of our recent paper [29]. The storage ring was operated under conditions of an electron beam energy of 750 MeV and a stored current of 200–100 mA. The beamline was equipped with a focusing pre-mirror and a double-crystal monochromator [30]. An elliptically bent cylindrical mirror coated with Pt was used as the pre-mirror in order to achieve both horizontal and vertical focusings at the sample position. For the measurements for the Ge and Se $2p_{3/2}$ core absorption spectra, beryl was used as the monochromator crystal, which provided soft x-rays from 830 to 1800 eV with a resolving power ($E/\Delta E$) of about 1500. For the Te $3p_{3/2}$ core absorption measurements, we used a β-alumina monochromator, which supplied soft x-rays from 600 to 1750 eV with a value of $E/\Delta E$ of about 1000. All of the core absorption spectra were taken in total-electron-yield mode at room temperature. The intensity of the incident beam was monitored using the photoelectric current of a Au mesh placed in front of the sample and this was used for normalization.

The core absorption measurements were carried out using two ultrahigh-vacuum chambers: a sample preparation one and an analyser one, operating under base pressures of 1.0×10^{-9} and 5.0×10^{-10} Torr, respectively. The sample preparation chamber was the same as that used for the UPS and IPES measurements, which is shown at the right-hand side of figure 3. The sample film of a-GeSe with the thickness of about 1000 Å was prepared *in situ* by evaporation onto a clean Au substrate in the preparation chamber using a quartz furnace. The a-GeTe sample film with the thickness of about 1000 Å was evaporated onto a Mo substrate in the preparation chamber. We used the same materials, with purity of 99.9999%, for evaporating sources for a-GeSe and a-GeTe as for the UPS and IPES measurements. The sample thickness was measured by means of deviations of the frequency of a quartz oscillator placed near the sample position. The evaporation rate for each film was set to about 0.5 Å s^{-1} in order to conserve the stoichiometry of the sample. The concentration of each film was later examined by means of an electron microprobe analysis. A clean surface of c-GeSe was obtained by cleaving a single crystal in the preparation chamber under an ultrahigh vacuum of about 3.0×10^{-10} Torr. The core absorption measurements for the c-GeSe sample were performed varying the angle of incidence of the soft x-rays, but no angle variation of the spectra was observed. A clean surface of c-GeTe was obtained by scraping a polycrystalline lump using a diamond file in the preparation chamber under the same vacuum conditions. The sample was transferred into the analyser chamber *in situ* under an ultrahigh vacuum below 5.0×10^{-10} Torr.
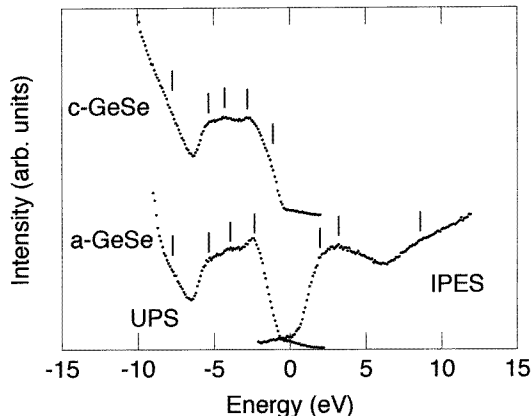
Figure 4. UPS and IPES spectra for a- and c-GeSe. Energies are defined with respect to the Fermi level. Vertical bars indicate the positions of peaks and shoulders.

3. Results

3.1. UPS and IPES spectra

Figure 4 shows the UPS and IPES spectra obtained for a- and c-GeSe. The energies are referred to the Fermi level. The UPS spectrum of a-GeSe has a relatively large peak at −2.4 eV, a small peak at −3.9 eV and a shoulder at around −5.4 eV in the Ge 4p and Se 4p region. The valence-band maximum (VBM) is at around −0.7 eV. This upper subband in the valence bands is separated by a steep dip at −6.5 eV from the lower Ge 4s subband at around −8 eV, which was clearly apparent in the XPS spectra taken by Oyanagi *et al* [6] and Theye *et al* [13]. The Ge 4s subband in the present UPS spectrum is, however, very blurred behind a strong background of secondary electrons, in contrast to the previous UPS data obtained by Hino, Takahashi and Harada [11]. Aside from the Ge 4s subband, however, our result is in excellent agreement with theirs; i.e., they obtained structures at −1.7, −3.3 and −4.6 eV with respect to the VBM, which are consistent with our data within the accuracy of the experiments. On the other hand, the −2.4 eV peak was not found in every XPS measurement [6, 13]. The photoionization cross section of Se 4p electrons for a He I exciting light source (21.2 eV) is calculated to be about 5.3 times larger than that of Ge 4p electrons, whereas the ratio for soft x-rays is about 3.5 [31]. Therefore, it is reasonable to suppose that the −2.4 eV peak mainly originates from Se 4p states.

The IPES spectrum of a-GeSe has a threshold of the conduction-band minimum (CBM) at around 0.7 eV. The band gap obtained from the two spectroscopies is about 1.4 eV, which is in good agreement with the optical absorption edge measured by Kotkata, Kandil and Theye [32]. A shoulder at around 1.9 eV and a broad peak at 3.2 eV are observed above the strong increase of the CBM threshold. These lower bands in the unoccupied states are well separated from a shoulder at around 8.5 eV by a clear dip at 6.3 eV.

In the UPS spectrum of c-GeSe, the form of the upper subband is very different from that for a-GeSe. The −2.4 eV peak seen for a-GeSe disappears and, in turn, two weak peaks at around −2.8 and −4.3 eV and a strong shoulder at −5.3 eV are generated on crystallization. In addition, the slope of the VBM threshold becomes gradual due to a weak shoulder at around −1.2 eV. A deep dip between the upper subband and the Ge 4s band is also observed at −6.4 eV. The Ge 4s band, however, is not clear, as expected from

the band calculations performed using pseudopotential [33] and LCAO methods [34, 35] and the XPS results [6, 13]. The present result is essentially in good agreement with the theoretical calculations, except that the -2.8 eV structure cannot be interpreted by any of the calculations. Taniguchi *et al* [36] performed angle-integrated UPS measurements using synchrotron radiation and obtained a distinct peak at -2.3 eV with respect to the VBM especially when the electric vector of the polarized synchrotron light was parallel to the crystal *a*-axis.
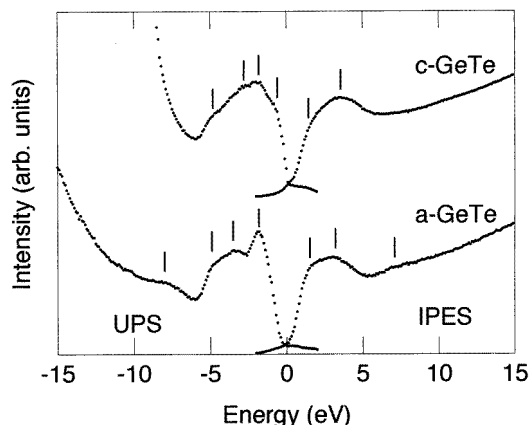

Figure 5. UPS and IPES spectra for a- and c-GeTe. Energies are defined with respect to the Fermi level. Vertical bars indicate the positions of peaks and shoulders.

Figure 5 shows the UPS and IPES spectra obtained for a- and c-GeTe. The energies are again defined with respect to the Fermi level. The basic features of the upper subband in the UPS spectra of a-GeTe are very similar to that for a-GeSe; it has a distinct peak at -1.8 eV, a small peak at -3.5 eV and a shoulder at around -4.9 eV in the Ge 4p and Te 5p region. The VBM is at around -0.3 eV. This upper subband in the valence bands is separated by a steep dip at -6.0 eV from the lower Ge 4s subband at around -8.0 eV. The whole UPS spectrum of the present study for a-GeTe is in excellent agreement with the previous data obtained by Schevchik *et al* [24], and Takahashi *et al* [12, 25]; i.e., they obtained structures at -1.6, -3.1 and -4.4 eV with respect to the VBM, which are consistent with our data within the accuracy of the experiments. The -1.8 eV peak was also found in every XPS measurement [12, 22–25]. This would be because the ratios of the photoionization cross sections of Te 5p and Ge 4p electrons are almost equal, about 3.2, for that using a He I light source and that using soft x-rays [31].

The IPES spectrum of a-GeTe has a threshold of the CBM at around 0.3 eV. Thus the band gap obtained from the two spectroscopies is about 0.6 eV, which is in good agreement with the optical absorption gap of 0.8 eV [37]. The shape of the IPES spectrum of a-GeTe is also very similar to that of a-GeSe. A shoulder at about 1.5 eV and a broad peak at 3.2 eV are observed above the strong increase of the CBM threshold. These lower bands in the unoccupied states are well separated from a shoulder at around 7.0 eV by a clear dip at 5.5 eV.

In the UPS spectrum of c-GeTe, the Fermi energy of the sample was located at the VBM. The form of the upper subband is very different from that for a-GeTe; the -1.8 eV peak becomes very small and broad, and fine structures at around -0.6, -2.8 and -4.8 eV form an upper subband from 0 to -6.0 eV. The basic features of the subband are similar

to those for c-GeSe, but the −0.6 and −4.8 eV shoulders are stronger and weaker than the corresponding −1.2 and −5.3 eV shoulders in the c-GeSe spectrum, respectively. A deep dip between the upper subband and the Ge 4s band also appears at −6.0 eV. Although the existence of a clear Ge 4s band was expected from the XPS results [12, 22–25] and band calculations carried out using an empirical pseudopotential method [38], a relativistic orthogonal plane-wave (OPW) method [39, 40] and an *ab initio* nonlocal relativistic pseudopotential method [41], it could not be observed due to a strong background of secondary electrons.

The IPES spectrum of c-GeTe has a threshold of the CBM at around 0.3 eV. Therefore the band gap obtained from the two spectroscopies is about 0.3 eV, which is much smaller than the optical absorption gap of about 0.8 eV and a little larger than that determined from the tunnelling spectroscopy of 0.1–0.2 eV [37]. The shape of the spectrum also differs from that of a-GeTe. A weak shoulder at about 1.4 eV and a very broad peak at 3.5 eV are observed above a gradual increase of the CBM threshold. It should be noticed that these lower bands in the unoccupied states are not well separated from the upper bands and there is no shoulder in higher bands as observed for a-GeTe. The present IPES spectrum is in relatively good agreement with the relativistic OPW calculation made by Ortenburger and Rudge [40]. The empirical pseudopotential calculation [38], however, gives a large inconsistency as regards the energy position of the DOS peaks in the conduction bands as well as in the valence bands, as shown by Shevchik *et al* [24].
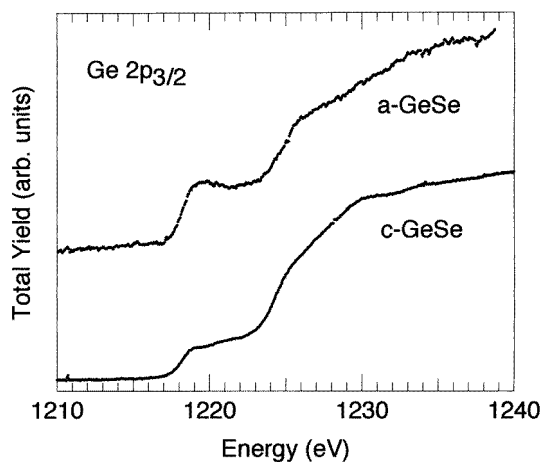

Figure 6. The Ge $2p_{3/2}$ core absorption spectra for a- and c-GeSe.

3.2. Soft-x-ray core absorption spectra

Figure 6 shows the Ge $2p_{3/2}$ core absorption spectra for a- and c-GeSe as functions of the soft-x-ray photon energy. The spectrum of a-GeSe has an edge at 1217 eV and a broad peak at around 1219 eV. From the selection rule for the angular momentum on the optical transition, it is readily supposed that these levels are mainly Ge 4s states; this was supported by some band calculations for a-Ge–Se mixtures [42, 43]. Again, at 1223.5 eV the absorption suddenly increases with increasing energy, and has a shoulder at 1225.5 eV. The spectrum obtained is in good agreement with the previous measurement made using a standard absorption method by Belin, Senemaud and Guita [44]. On the other hand, the

spectrum of c-GeSe is definitely different from that of a-GeSe, especially in the low-energy region. Although the energy position of the threshold is almost the same, the magnitude of the absorption from 1217 to 1223 eV is very small. This difference suggests that c-GeSe has far fewer unoccupied levels with Ge s and/or d character than a-GeSe in the bottom 6 eV of the conduction bands. The spectrum in the high-energy region beyond 1224 eV, on the other hand, indicates the same trend as for a-GeSe, except the different location of some small shoulders.
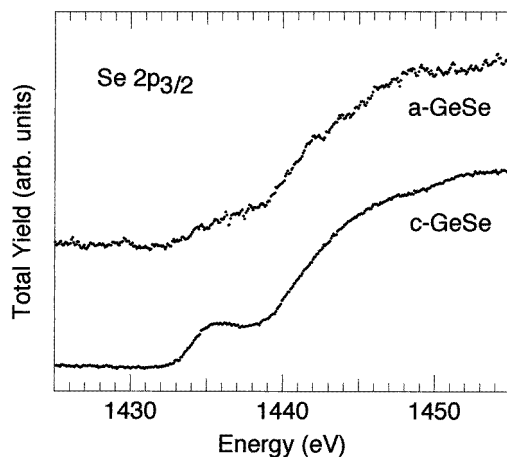

Figure 7. The Se $2p_{3/2}$ core absorption spectra for a- and c-GeSe.

Figure 7 shows the Se $2p_{3/2}$ core absorption spectra for a- and c-GeSe as functions of the soft-x-ray photon energy. The spectrum of a-GeSe has a blurred edge at 1433 eV, and gradually increases up to about 1439 eV with increasing energy. From the selection rule for the angular momentum on the optical transition, it is readily supposed that these levels are mainly Se 4s states; this was supported by some band calculations for a-Ge–Se mixtures [42, 43]. Beyond 1439 eV the absorption shows a sudden and strong increase and has a shoulder at 1449 eV. The spectrum obtained is in good agreement with the previous measurement made using a standard absorption method by Belin, Senemaud and Guita [44]. On the other hand, the spectrum of c-GeSe is definitely different from that of a-GeSe, especially in the low-energy region. The magnitude of the absorption from 1433 to 1439 eV is very large and a clear shoulder appears at around 1435.5 eV. This difference suggests that c-GeSe has more unoccupied levels with Se s and/or d character than a-GeSe in the bottom 6 eV of the conduction bands. The spectrum in the high-energy region beyond 1439 eV, on the other hand, indicates almost the same trend as for a-GeSe.

Figure 8 exhibits the Ge $2p_{3/2}$ core absorption spectra for a- and c-GeTe as functions of the soft-x-ray photon energy. The spectrum of a-GeTe has an edge at 1217 eV and a broad peak at around 1219 eV. From the selection rule, it is readily supposed that these levels are mainly Ge 4s states. Again, at 1222 eV the absorption suddenly increases with increasing energy, and has a shoulder at 1226 eV. The magnitude of the spectrum of c-GeTe from 1217 to 1222 eV is very small compared with that of a-GeTe, which suggests that c-GeTe has fewer unoccupied levels with Ge s and/or d character than a-GeTe in the bottom 5 eV of the conduction bands. The spectrum in the high-energy region beyond 1222 eV, on the other hand, indicates the same trend as for a-GeTe.
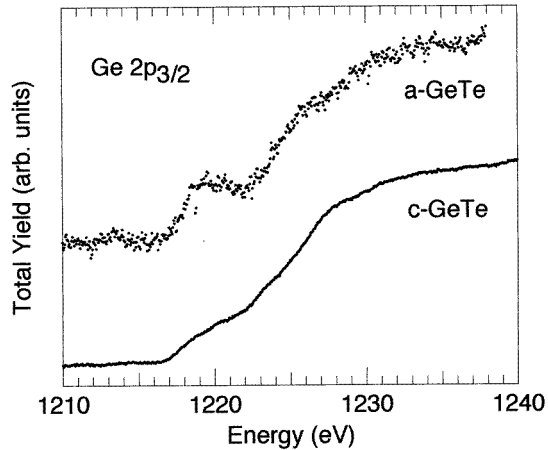
Figure 8. The Ge $2p_{3/2}$ core absorption spectra for a- and c-GeTe.
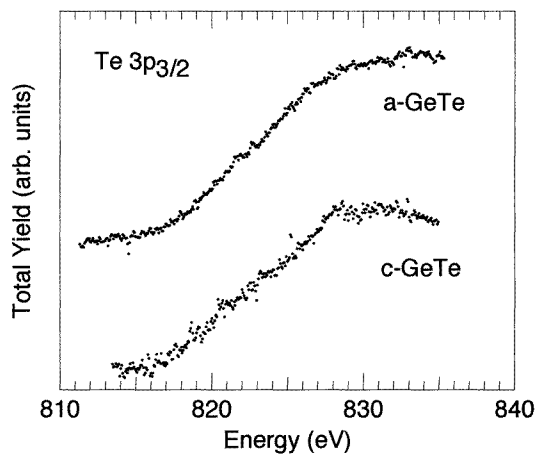

Figure 9. The Te $3p_{3/2}$ core absorption spectra for a- and c-GeTe.

Figure 9 exhibits the Te $3p_{3/2}$ core absorption spectra for a- and c-GeTe as functions of the soft-x-ray photon energy. Both of the spectra are almost structureless and increase monotonically with energy. The difference between them is small, especially in the lower-energy range around 820 eV.

4. Discussion

In this section, we give a discussion of the local configuration, divided into two subsections on a-GeSe and a-GeTe.

4.1. Amorphous GeSe

O'Reilly, Robertson and Kelly [10] carried out calculations of the DOS for the 3(Ge):3(Se)- and 4(Ge):2(Se)-coordinated networks of a-GeSe. For the 3(Ge):3(Se) coordination, the

calculation was performed for the Matthews–Davis–Elliott model with rings with even numbers of atoms. For the 4(Ge):2(Se) coordination, a-GeSe networks with and without chemical order were simulated using a tight-binding method. The calculations were made in the wide-valence-band region and over a short energy range (5 eV) of the conduction band.

In order to compare them with our experimentally obtained UPS and IPES spectra in detail, we have to make the correction of subtracting the backgrounds from the spectra. They are mainly produced by the inelastic electron scattering occurring in the process of photoemission or inverse photoemission. For the UPS spectra, we used the simplest 'integral' method, which was first proposed by Shirley [45]. The main assumption of this method is that the electron energy-loss spectrum has a constant tail towards the low-energy side. We chose the magnitude of the inelastic tail to be 7% eV^{-1} for the UPS spectrum of a-GeSe so that the minimum at around −6 eV in our corrected experimental spectrum almost coincides with each of the broadened theoretical DOSs. The theoretical DOSs were broadened by two functions. One was a Gaussian function with the standard deviation of the experimental resolution equal to 0.2 eV and the other was a Lorentzian function included to take the electron lifetime into account. The gamma parameter of the Lorentzian was chosen as in the literature [46].

For the background correction of the IPES spectra, many methods have been proposed as reported by Goodman and Henrich [47]. They concentrated on ways of considering the inelastic scattering of the incident electron beam—such as by using the electron energy-loss spectra (EELS) obtained, theoretical calculation of the production of electron–hole pairs, or a Monte Carlo simulation. But it is still open to discussion, as mentioned in the above-cited literature. We, therefore, used the simplest and empirical integral model, with a constant inelastic tail, because EELS spectra of a-GeSe and GeTe are not available and our discussion is limited to the low-energy region near the Fermi level. Turtle and Liefeld removed the inelastic background of the x-ray IPES spectrum by using a measured XPS spectrum [48]. They assumed that the photoemission spectrum of a narrow core level and its inelastic tail approximate the inelastic spectrum of electrons produced by an incident monoenergetic electron beam in the IPES process if the kinetic energy of the photoemitted electron is nearly equal to that of the incident electron beam. We also assumed that the inelastic tail in the IPES process was the constant tail as used for the correction of our UPS spectrum, namely 7% eV^{-1}. For the comparison, the theoretical DOSs were also broadened by a real resolution function of this equipment presented by Ueda *et al* [27] and the Lorentzian function.

Figure 10 shows the corrected UPS and IPES spectra (a) of a-GeSe together with the broadened theoretical DOS for (b) a 3(Ge):3(Se)-coordinated, (c) a *chemically ordered* (CO) and (d) a *randomly bonded* (RB) 4(Ge):2(Se)-coordinated network model [10]. In the figure, the energies of each spectrum are adjusted at the VBM and shown with respect to the Fermi level of the experimental data. As for the UPS spectrum, the local configuration in the a-GeSe has already been discussed, and it is clear that the existence of the −2.4 eV peak is not the evidence of 4(Ge):2(Se)-coordinated structure. The strong increase of the UPS spectrum below −7 eV might be due to the strong enhancement of the inelastic scattering of low-energy electrons, which was not taken into account within the framework of our present integral correction with a constant tail.

The corrected IPES spectrum for a-GeSe has a broad peak at around 3.0 eV and a shoulder at around 1.9 eV. These structures may be due to antibonding states of the covalent bonds in a-GeSe, and spread widely up to a dip at 6.3 eV. On the other hand, the energy range of the s and p antibonding orbitals of the theoretical DOS for the 3(Ge):3(Se) coordination
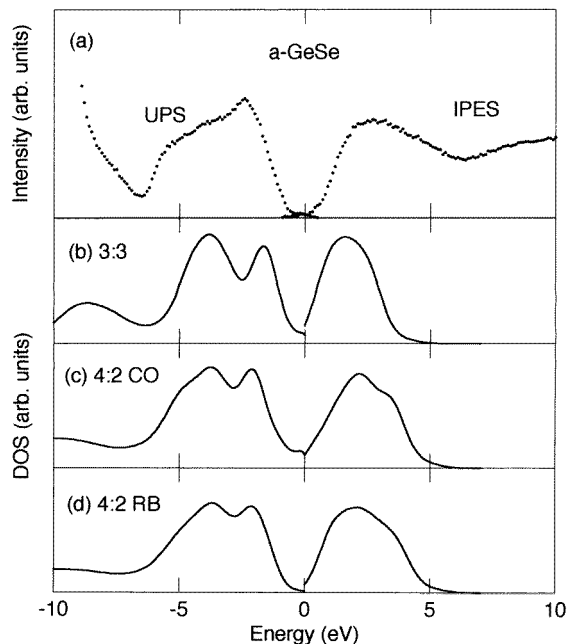
Figure 10. The corrected UPS and IPES spectra of a-GeSe (a) together with the broadened theoretical DOSs for (b) a 3(Ge):3(Se)-coordinated, (c) a *chemically ordered* (CO) and (d) a *randomly bonded* (RB) 4(Ge):2(Se)-coordinated network model [10]. For details, see the text.

is less than 4 eV, which may originate from the character of the model—i.e. the fact that the 3(Ge):3(Se) network is constructed solely from one type of Ge–Se unlike bond. In contrast, the results obtained with the 4(Ge):2(Se) models with both the *chemically ordered* and *randomly bonded* networks show relatively wide energy ranges of the antibonding states of around 5 eV. In each 4(Ge):2(Se) model, many Ge–Ge bonds are involved in the network. The tight-binding calculation by Bergignat *et al* [42] revealed that the energy range of the bonding state of the $Ge(Se_{1/2})_3Ge_{1/2}$ tetrahedron included in a-GeSe is much wider than that of the $Ge(Se_{1/2})_4$ tetrahedron existing in a-GeSe$_2$. This theoretical result also seems to support the broadening of the antibonding states.

It is useful to discuss the positions and intensities of the peaks in the calculated DOSs and the IPES spectrum. As seen in figure 10(b), the broadened theoretical DOS for the 3(Ge):3(Se) configuration has a large and broad peak at around 1.6 eV and a very small shoulder of 2.6 eV. The IPES spectrum obtained, however, shows a completely different form. In contrast, the theoretical DOS for the *chemically ordered* 4(Ge):2(Se) network model shown in figure 10(c) has a peak at 2.2 eV and a strong shoulder at 3.4 eV. The theoretical DOS for the *randomly bonded* 4(Ge):2(Se) network model shown in figure 10(d) has a broad peak at around 2.1 eV and two shoulders at 1.3 and 3.6 eV. The distinct difference from the *chemically ordered* 4(Ge):2(Se) coordination model is the existence of the strong shoulder in the low-energy range, which is not observed in the experimental IPES spectrum. Therefore, it should be concluded from the IPES spectrum that the *chemically ordered* 4(Ge):2(Se) coordination model is the most appropriate for the local structure in a-GeSe. However, it should also be noted that the 3.0 eV peak could not be reproduced using any of the models. Both *chemically ordered* and *randomly bonded* 4(Ge):2(Se) show

a hollow or a monotonic slope at around 3.0 eV. We believe that these models could not reproduce the 3.0 eV peak even if the Ge and Se 4d contributions tailing off from the higher-energy side were to be subtracted.
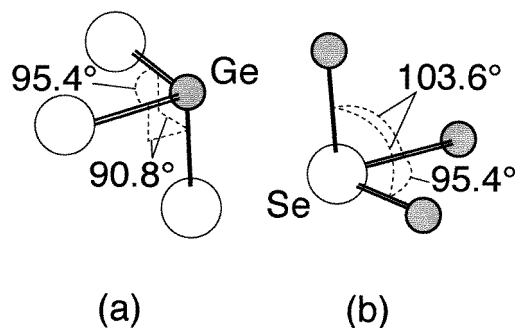

Figure 11. A drawing of the local coordination around (a) Ge and (b) Se atoms in orthorhombic GeSe [1].

As noted in the last section, both the Ge and Se $2p_{3/2}$ core absorption spectra of GeSe show distinct differences between the amorphous and crystalline phases, especially in the lowest 6 eV energy range. Figure 11 shows the local configuration around (a) Ge and (b) Se atoms in c-GeSe determined from an x-ray diffraction measurement by Okazaki [1]. Both the Ge and the Se atoms have three nearest neighbours of unlike atoms with almost the same bond lengths: 2.537 Å (single lines) and 2.582 Å (double lines). As seen in figure 11(a), Se atoms around a Ge atom are located with the bond angles of 90.8° and 95.4°—nearly right angles. For this configuration the bonding state of the Ge atom can be composed of pure 4p electrons, and need not hybridize with the 4s electrons. Therefore, it is reasonable that the Ge $2p_{3/2}$ core absorption spectrum is very weak in the low-energy range from 1217 to 1223 eV, which corresponds to the region of the Ge–Se antibonding states.

On the other hand, as seen in figure 11(b), Ge atoms around an Se atom are located with the bond angles of 95.4° and 103.6°, which are not near to being right angles. In order to form such a configuration, s or d electrons must get mixed with Se 4p electrons to enlarge the bond angle. Therefore, it is reasonable that the Se $2p_{3/2}$ core absorption spectrum for c-GeSe has a distinct structure in the low-energy range from 1433 to 1439 eV, which originates from the 4s states near the bottom of the conduction band.

The local structures of the typical 4(Ge):2(Se)-coordinated a-GeSe$_2$ around the Ge and Se atoms are shown in figure 12. The values of the bond angles are results from an anomalous x-ray scattering measurement made by Fuoss *et al* [5]. As seen in figure 12(a), Ge atoms are surrounded by four Se atoms with the bond angle of 109.5°, which is equal to the ideal bond angle of a tetrahedron, and almost the same as the average value of the corresponding bond angles in the high-temperature phase of c-GeSe$_2$ with a monoclinic form, 109.3° [49]. As is well known, the Ge 4s and 4p electrons should hybridize into sp^3 bonding states in order to form this local configuration with fourfold coordination. On the other hand, the bond angle around Se atoms is around 90°, which is almost the same as the corresponding averaged bond angles in c-GeSe$_2$ [49]. For this configuration, Se atoms can make two bonds with 4p electrons without the help of s or d electrons.

We have already taken Ge and Se $2p_{3/2}$ core absorption spectra of a-GeSe$_2$ [29] under the same conditions as for the present measurements, the results of which are shown in figure 13. In the Ge $2p_{3/2}$ core absorption spectrum of a-GeSe$_2$, a small peak at around
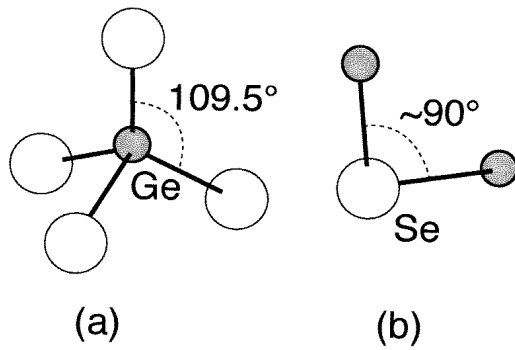
Figure 12. A drawing of the averaged local coordinations around (a) Ge and (b) Se atoms in the typical 4(Ge):2(Se)-coordinated a-GeSe$_2$ obtained from an anomalous x-ray scattering measurement [5].
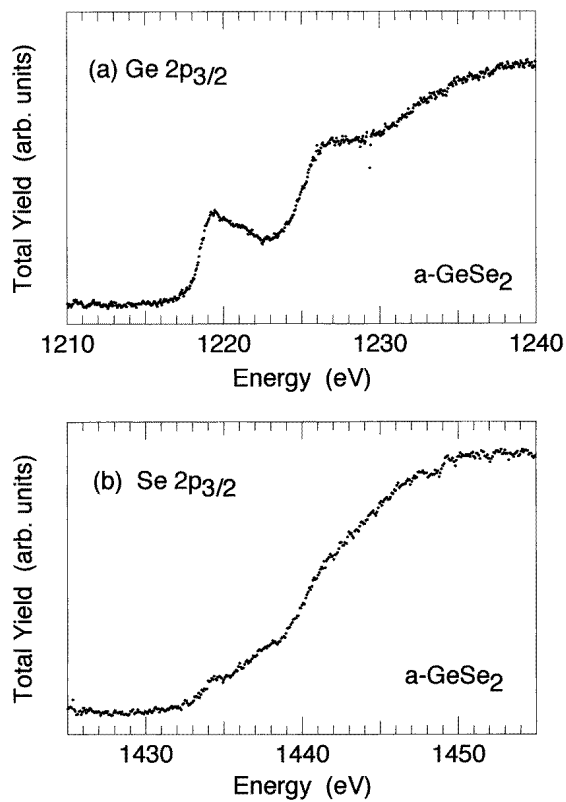

Figure 13. (a) Ge and (b) Se 2p$_{3/2}$ core absorption spectra of a-GeSe$_2$ [29].

1219 eV follows a sudden threshold at around 1218 eV. After that, the spectrum has a minimum at around 1223 eV and a shoulder at around 1226 eV. In the recent papers [28, 29], we have argued that the final states of the absorption in the energy range from 1218 to 1223 eV are mainly the Ge 4s states near the bottom of the conduction band, and those beyond 1223 eV mainly Ge 4d and/or 5s states. The Se 2p$_{3/2}$ core absorption spectrum

of a-GeSe$_2$ shows a gradual increase above a threshold at around 1433 eV. After that, a remarkable increase starts at around 1439 eV, a shoulder appears at around 1441 eV and the yield saturates at around 1450 eV. We have attributed the final states of the absorption in the energy range from 1433 to 1439 eV as mainly Se 4s states near the bottom of the conduction band, and those beyond 1439 eV as mainly Se 4d and/or 5s states. Our proposal was strongly supported by a recent band calculation by Pollard [50].

As clearly seen in figure 13(a), the Ge 2p$_{3/2}$ core absorption spectrum for a-GeSe is similar to that for a-GeSe$_2$, although the energy position of each structure in the a-GeSe$_2$ spectrum is about 1 eV higher than that in a-GeSe; this difference could originate from that of the band-gap energies [32]. This similarity strongly suggests that the bonding nature of the Ge atoms in a-GeSe is that of a sp^3 hybridization electronic configuration with a fourfold coordination. The Se 2p$_{3/2}$ core absorption spectrum for a-GeSe is very similar to that for a-GeSe$_2$ as shown in figure 13(b), which strongly suggests that the bonding nature of the Se atoms in a-GeSe is a simple p bonding with a twofold coordination. Therefore, the core absorption spectra strongly support a 4(Ge):2(Se) local coordination in a-GeSe.

Belin, Senemaud and Guita [44] recorded Ge and Se 2p$_{3/2}$ core absorption spectra of a-GeSe using the usual absorption method, and proposed that the coordination in a-GeSe might be mainly 3(Ge):3(Se) because the edge at the bottom of the conduction band is relatively abrupt and spreads over about 1 eV in both the experimental Ge 2p$_{3/2}$ curve and the calculated result for the 3(Ge):3(Se) coordination [10]. Such a trend in the experimental spectrum was also seen in our present work. However, as they also stated in their report, the p core spectrum does not show the total conduction-band DOS as the result of the calculations, but the s and/or d contributions. Therefore, their speculation was not firmly grounded.

Consequently, all of the measurements discussed here indicate that the *chemically ordered* 4(Ge):2(Se) coordination model is more appropriate for a-GeSe, although a *randomly bonded* 4(Ge):2(Se) configuration structure still remains a possibility.

4.2. Amorphous GeTe

Although the local coordinations in a-GeTe are still open to argument, almost all studies have indicated that the bonding natures of the amorphous phases are somewhat different from that of c-GeTe; this is also the conclusion of recent work using newly developed techniques. Fukui *et al* took ultraviolet core absorption [51] and UPS [52] spectra for a-GeTe using synchrotron radiation and found that the contribution of the Te 5p state to the conduction band is larger in the amorphous phase than in the crystalline phase and, thus, the covalency of the Ge–Te bonds is stronger in the amorphous phase than in the crystalline phase.

Figure 14 shows the corrected UPS and IPES spectra (a) of a-GeTe together with the broadened theoretical DOS for (b) a 3(Ge):3(Te)-coordinated, (c) a *chemically ordered* (CO) and (d) a *randomly bonded* (RB) 4(Ge):2(Te)-coordinated network model [10]. Corrections of the UPS and IPES spectra were carried out along the same lines as for a-GeSe. We chose the constant inelastic tail of 7% eV^{-1}. In the figure, the energies of each spectrum are adjusted at the VBM and shown with respect to the Fermi level of the experimental data. As for the UPS spectrum, O'Reilly, Robertson and Kelly [10] have already discussed the local configuration in a-GeTe on the same basis as for a-GeSe, and it has been established that the existence of the −1.8 eV peak is not the evidence of a 4(Ge):2(Te)-coordinated structure.

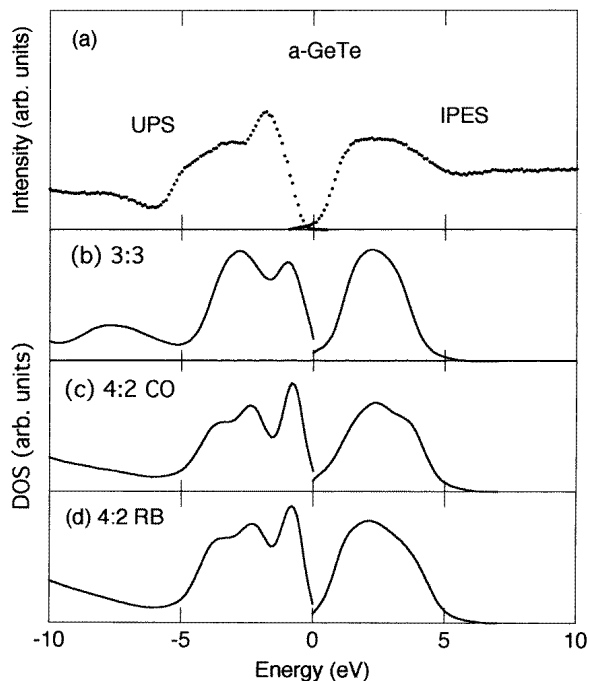The corrected IPES spectrum for a-GeTe has two shoulders at around 1.5 and 3.1 eV in

Figure 14. The corrected UPS and IPES spectra of a-GeTe (a) together with the broadened theoretical DOSs for (b) a 3(Ge):3(Te)-coordinated, (c) a *chemically ordered* (CO) and (d) a *randomly bonded* (RB) 4(Ge):2(Te)-coordinated network model [10]. For details, see the text.

the vicinity of the broad peak at around 2.2 eV. These structures may be due to antibonding states of the covalent bonds in a-GeTe, and spread widely up to a dip at 5.5 eV. On the other hand, the energy range of the s and p antibonding orbitals of the theoretical DOS for the 3(Ge):3(Te) coordination is only 4.5 eV; this is the case because in the model the 3(Ge):3(Te) network is constructed solely from one type of Ge–Te unlike bond. In contrast, the 4(Ge):2(Te) models with both *chemically ordered* and *randomly bonded* networks show relatively wide energy ranges of the antibonding states of around 5 eV. In each 4(Ge):2(Te) model, many Ge–Ge bonds are involved in the network.

It is also useful to discuss the positions and intensities of the peaks in the calculated DOSs and the IPES spectrum. As seen in figure 14(b), the broadened theoretical DOS for the 3(Ge):3(Te) configuration has a large and broad peak at around 2.3 eV and a small shoulder at 3.0 eV. The IPES spectrum obtained, however, has the strong shoulder at 1.5 eV. The broadened theoretical DOS for the *chemically ordered* 4(Ge):2(Te) network model in figure 14(c) has a peak at 2.5 and a strong shoulder at 3.6 eV, but no peak or shoulder at around 1.5 eV. It is impossible to reproduce the experimental IPES spectrum from these theoretical DOSs. In contrast, the broadened theoretical DOS for the *randomly bonded* 4(Ge):2(Te) network model in figure 14(d) has a broad peak at around 2.2 eV with shoulders of 1.4 and 3.8 eV. This calculated DOS is in good agreement with the experimental IPES result if the 1.4 eV shoulder becomes slightly larger and the tail of the Ge 4d and Te 5d contributions from the higher-energy range is taken into account. Therefore, it should be concluded from the IPES spectrum that the *randomly bonded* 4(Ge):2(Te) coordination model is the most appropriate for the local structure in a-GeTe.

As noted in the last section, the Ge $2p_{3/2}$ core absorption spectra of GeTe show a distinct difference between the amorphous and crystalline phases, especially in the lowest 5 eV energy range. As shown in figure 2, each Ge or Te atom in the crystal phase is surrounded by six unlike atoms with three short and three long bonds of lengths 2.84 Å (solid lines) and 3.17 Å (dashed lines), respectively. For such a NaCl-type local configuration, it is normal to consider that the bondings are constructed of d^2sp^3 hybridization states, and that s and d states get mixed into the antibonding states in the conduction bands. A recent *ab initio* relativistic pseudopotential calculation [41], however, revealed that the lowest conduction band is predominantly Ge p-like in c-GeTe. According to the band calculation, therefore, it is reasonable that both the Ge $2p_{3/2}$ and Te $3p_{3/2}$ core absorption spectra show weak absorptions in the lowest 5 eV energy ranges, as seen in figures 8 and 9, respectively.

On the other hand, the Ge $2p_{3/2}$ core absorption spectrum of a-GeTe is definitely different from that of c-GeTe, and very similar to that of a-GeSe shown in figure 7. As mentioned above in the discussion of a-GeSe, the form of the Ge $2p_{3/2}$ core absorption spectrum strongly indicates sp^3 hybridization of the bonding states; this is evidence for fourfold coordination of the Ge atoms. The difference between the Te $3p_{3/2}$ core absorption spectra of a- and c-GeTe, on the other hand, could not be clearly seen in the present study because of the rather scattered data. Källne and Ribbing [53] took Te 2s and $2p_{3/2}$ core absorption spectra for a- and c-GeTe and found that the d-like states at 5–10 eV above the absorption edge increase a little on going from a crystalline to an amorphous phase, whereas the lower sp bands remain unchanged. The same trend seems to apply also in the present Te $3p_{3/2}$ core absorption spectra. Although the differences of the Te p core absorption spectra are very small and ambiguous, it would be reasonable to speculate that the Te 5d electrons in the crystal, which get mixed with 5s and 5p electrons to give rise to the d^2sp^3 hybridized states and sixfold coordination of the Te atoms, return to the original energy positions upon amorphization, because of the reduction of the coordination number around the Te atoms down to 2 as suggested in a number of previous studies of the local structure in a-GeTe.

Consequently, all of the measurements considered here indicate that the *randomly bonded* 4(Ge):2(Te) coordination model is more appropriate for a-GeTe.

5. Summary

The valence- and conduction-band electronic DOSs in a-GeSe and GeTe were investigated by means of UPS and IPES, respectively. The UPS spectra for both a-GeSe and a-GeTe are very similar to those obtained in previous experiments; a distinct peak appears near the top of the valence band. The corrected IPES spectra for both a-GeSe and GeTe exclude the possibility of a 3(Ge):3(chalcogen)-coordinated structure if one compares them with the broadened theoretical DOS calculated by O'Reilly, Robertson and Kelly. The corrected IPES spectrum for a-GeSe shows a fairly similar trend to the corresponding broadened theoretical DOS for *chemically ordered* 4(Ge):2(Se) structure, whereas for a-GeTe the similarity is to the trend shown by *randomly bonded* 4(Ge):2(Te) structure. The characters of the conduction-band DOS for a-GeSe and a-GeTe were also examined by means of soft-x-ray core absorption spectroscopy. The Ge and Se $2p_{3/2}$ core absorption spectra of a-GeSe are very similar to those of a-GeSe$_2$, and were discussed using a simple bonding model with a 4(Ge):2(Se) local configuration. The Ge $2p_{3/2}$ and Te $3p_{3/2}$ core absorption spectra of a-GeTe were also discussed using a simple local bonding model. All of the measurements considered here indicated that both a-GeSe and a-GeTe have 4(Ge):2(chalcogen)-coordinated structures.

Acknowledgments

References

[1] Okazaki A 1958 *J. Phys. Soc. Japan* **13** 1151
[2] Goldak J, Barrett C S, Iness D and Youdelis W 1966 *J. Chem. Phys.* **44** 3323
[3] Sayers D E, Lytle F W and Stern E A 1972 *J. Non-Cryst. Solids* **8–10** 401
[4] Uemura O, Sagara Y and Satow T 1974 *Phys. Status Solidi* a **26** 99
[5] Fuoss P H, Eisenberger P, Warburton W K and Bienenstock A 1981 *Phys. Rev. Lett.* **46** 1537
[6] Oyanagi H, Tanaka K, Hosoya S and Minomura S 1981 *J. Physique Coll.* **42** C4 221
[7] Kawamura H and Matsumura M 1980 *J. Non-Cryst. Solids* **35+36** 1215
[8] Chamberlain J M, Sirbegovic S S and Nikolic P M 1974 *J. Phys. C: Solid State Phys.* **7** L150
[9] Trodahl H J 1982 *Solid State Commun.* **44** 319
[10] O'Reilly E P, Robertson J and Kelly M J 1981 *Solid State Commun.* **38** 565
[11] Hino S, Takahashi T and Harada Y 1980 *Solid State Commun.* **35** 379
[12] Takahashi T and Sagawa T 1983 *J. Non-Cryst. Solids* **59+60** 879
[13] Theye M-L, Gheorghiu A, Senemaud C, Kotkata M F and Kandil K M 1994 *Phil. Mag.* B **69** 209
[14] Betts F, Bienenstock A and Ovshinsky S R 1970 *J. Non-Cryst. Solids* **4** 554
[15] Dove D B, Heritage M B, Chopra K L and Bahl S K 1970 *Appl. Phys. Lett.* **16** 138
[16] Uemura O, Sagara Y, Tsushima M, Kamikawa T and Satow T 1979 *J. Non-Cryst. Solids* **33** 71
[17] Pickart S J, Sharma Y P and de Neufville J P 1979 *J. Non-Cryst. Solids* **34** 183
[18] Maeda Y and Wakagi M 1991 *Japan. J. Appl. Phys.* **30** 101
[19] Fisher G B, Tauc J and Verhelle Y 1974 *Amorphous and Liquid Semiconductors* ed J Stuke (London: Taylor and Francis) p 1259
[20] Boolchand P, Triplett B B, Hanna S S and de Neufville J P 1974 *Mössbauer Effect Methodology* (New York: Plenum)
[21] Fisher G B and Spicer W E 1972 *J. Non-Cryst. Solids* **8–10** 978
[22] Fisher G B, Lindau L, Orlowski B A, Spicer W E, Verhelle Y and Weaver H E 1974 *Amorphous and Liquid Semiconductors* ed J Stuke (London: Taylor and Francis) p 621
[23] Schevchik N J, Tejeda J, Langer D W and Cardona M 1973 *Phys. Rev. Lett.* **30** 659
[24] Schevchik N J, Tejeda J, Langer D W and Cardona M 1973 *Phys. Status Solidi* b **57** 245
[25] Takahashi T, Sakurai H and Sagawa T 1982 *Solid State Commun.* **44** 723
[26] Yokoyama K, Nishihara K, Mimura K, Hari Y, Taniguchi M, Ueda Y and Fujisawa M 1993 *Rev. Sci. Instrum.* **64** 87
[27] Ueda Y, Nishihara K, Mimura K, Hari Y, Taniguchi M and Fujisawa M 1993 *Nucl. Instrum. Methods* A **330** 140
[28] Hosokawa S, Nishihara K, Hari Y, Taniguchi M, Matsuda O and Murase K 1993 *Phys. Rev.* B **47** 15 509
[29] Hosokawa S, Kouchi T, Ono I, Taniguchi M, Takata Y and Kosugi N 1996 *J. Phys.: Condens. Matter* **8** 1607
[30] Hiraya A, Horigome T, Okada N, Mizutani N, Sakai K, Matsudo O, Hasumoto M, Fukui K and Watanabe M 1992 *Rev. Sci. Instrum.* **63** 1264
[31] Yeh J J and Lindau I 1985 *At. Data Nucl. Data Tables* **32** 1
[32] Kotkata M F, Kandil K M and Theye M-L 1993 *J. Non-Cryst. Solids* **164–166** 1259
[33] Valiukonis G, Gashimzade F M, Guseinova D A, Krivaite G, Kulibekov A M, Orudzhev G S and Sileika A 1983 *Phys. Status Solidi* b **117** 81
[34] O'Reilly E P 1982 *J. Phys. C: Solid State Phys.* **15** 1449
[35] Gashimzade F M, Guliev D G, Guseinova D A and Shteinshrayber V Y 1992 *J. Phys.: Condens. Matter* **4** 1081
[36] Taniguchi M, Johnson R L, Ghijsen J and Cardona M 1990 *Phys. Rev.* B **42** 3634
[37] Bahl S K and Chopra K L 1969 *J. Appl. Phys.* **40** 4940
Bahl S K and Chopra K L 1970 *J. Appl. Phys.* **41** 2196
[38] Tung Y W and Cohen M L 1969 *Phys. Rev.* **180** 823

[39] Herman F, Kortum R L, Ortenburger I B and van Dyke P 1968 *J. Physique Coll.* **29** C4 62
[40] Ortenburger I B and Rudge W E 1973 *Bull. Am. Phys. Soc.* **18** 323
       The figure showing their calculation results was cited in reference [22].
[41] Robe K K and Joannopoulos J D 1987 *Phys. Rev.* B **36** 3319
[42] Bergignat E, Hollinger G, Chermette H, Pertosa P, Lohez D, Lannoo M and Bensoussan M 1988 *Phys. Rev.* B **37** 4506
[43] Lannoo M and Bensoussan M 1977 *Phys. Rev.* B **16** 3546
[44] Belin E, Senemaud C and Guita S 1991 *Phil. Mag.* B **63** 1159
[45] Shirley D A 1972 *Phys. Rev.* B **5** 4709
[46] Shimada K, Saitoh T, Namatame H, Fujimori A, Ishida S, Asano S, Matoba M and Anzai S 1996 *Phys. Rev.* B **53** 7673
[47] Goodman K W and Henrich V E 1994 *Phys. Rev.* B **49** 4827
[48] Turtle R R and Liefeld R J 1973 *Phys. Rev.* B **7** 3411
[49] Von Dittmer G and Schäfer H 1976 *Acta Crystallogr.* B **32** 2726
[50] Pollard W 1992 *J. Non-Cryst. Solids* **144** 70
[51] Fukui K, Saito T, Kondo S, Fujii Y, Sakisaka Y and Watanabe M 1990 *J. Phys. Soc. Japan* **59** 4161
[52] Fukui K 1992 *J. Phys. Soc. Japan* **61** 1084
[53] Källne E and Ribbing C-G 1975 *J. Phys. C: Solid State Phys.* **8** 2953